3D Dubins Path for Close-Range Cases: In the Application of Steerable Needles

Mengyu Fu[1]

***Abstract*— Being able to take 3D curvilinear trajectories, steerable needles can move around critical anatomical structures and precisely reach clinically significant targets in a minimally invasive way. Motion planning for steerable needle has been studied to automatically generate obstacle-free, kinematically feasible, and low targeting error trajectories for needles to follow. For steerable needles, a trajectory is kinematically feasible if the curvatures along it is bounded by some maximum curvature $\kappa_{\max}$. Unlike the case in 2D, planning bounded-curvature trajectories in 3D still remains an open question. More specifically, it is unclear under what condition a bounded-curvature trajectory between two configurations exists and how to compute a bounded-curvature trajectory given two "reachable" configurations. In this work, we consider so-called "close-range reachability" for bounded-curvature trajectories in 3D, where the trajectory length is comparable to the minimum radius of curvature $r_{\min} = \frac{1}{\kappa_{\max}}$ (unlike the cases of car driving where the distance to travel is much longer than the turning radius). We provide the definition of *closely reachable configurations* and give a proof sketch for the sufficient and necessary conditions for two configurations to be closely reachable. We also provide a numerical method to compute a bounded-curvature trajectory between two closely reachable configurations.**

I. Close-Range Reachability

In this section, we first introduce the notion of *closely reachable configurations* and provide a proof sketch to state the sufficient and necessary conditions for two configurations to be closely reachable.

Definition 1 (Closely reachable configuration)**.** Let $\mathbf{x}_0, \mathbf{x}_1 \in \mathcal{X}^*$ be two configurations and $\kappa_{\max}$ be the maximum curvature. Let $r_{\min} = 1/\kappa_{\max}$ be the minimum radius of curvature. We say $\mathbf{x}_1$ is a closely reachable configuration of $\mathbf{x}_0$ if

(i) $\|\text{Pos}(\mathbf{x}_1) - \text{Pos}(\mathbf{x}_0)\|_2 \leq 2r_{\min}$, where $\text{Pos}(\mathbf{x}) \in \mathbb{R}^3$ is the translation part of $\mathbf{x}$, and

(ii) there exists some bounded-curvature trajectory, whose length is no longer than $\pi r_{\min}$, that starts from $\mathbf{x}_0$ and terminates at $\mathbf{x}_1$.

Denote the two configurations we are considering as $\mathbf{x}_0$ and $\mathbf{x}_1$, and we have $\mathbf{x}_i = (p_i, q_i)$ representing the translation and orientation of the configuration. We start with an outline of the proof. We start with defining a region of 3D points

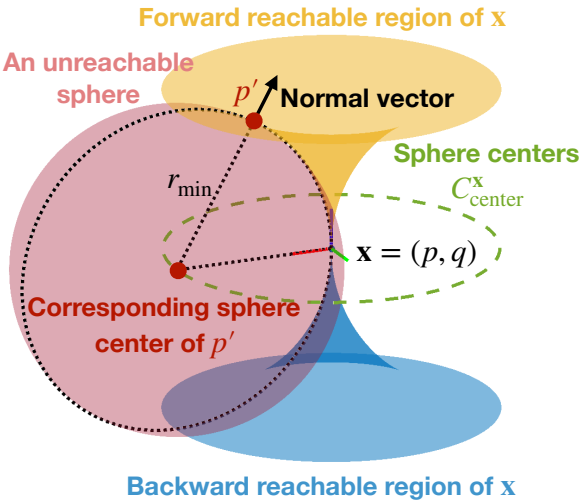

Fig. 1: Illustration of the forward and backward reachable regions associated with configuration $\mathbf{x}$. We additionally show an example of unreachable sphere and the circular curve $C^{\mathbf{x}}_{\text{center}}$.

that are closely reachable for a given configuration. It is obvious that for any configuration with p_1 to be reachable from $\mathbf{x}_0$, p_1 should lie in the forward reachable region of the source configuration $\mathbf{x}_0$. Similarly, p_0 should lie in the backward reachable region of the target configuration $\mathbf{x}_1$. By simultaneously considering the forward reachable region of $\mathbf{x}_0$ and the backward reachable region of $\mathbf{x}_1$, we argue that there must be a connected region, in the intersection of the two reachable regions, that includes both p_0 and p_1. We finally show that as long as such a connected region exists, we will be able to construct a curvature-bounded trajectory, with limited length, that connects $\mathbf{x}_0$ and $\mathbf{x}_1$.

Lemma 1 (Forward reachable region)**.** *Consider a configuration $\mathbf{x} = (p, q)$ where $p = (0, 0, 0)$ and $q = (1, 0, 0, 0)$. Then all closely reachable configurations of $\mathbf{x}$, lie in a trumpet-like region defined as the collection of points $(x, y, z) \in \mathbb{R}^3$ such that*

$$\begin{aligned}
&\forall \alpha \in [0, 2\pi), \beta \in [0, \pi], \\
&x = r_{\min} \cdot (1 - \cos\beta) \cdot \cos\alpha, \\
&y = r_{\min} \cdot (1 - \cos\beta) \cdot \sin\alpha, \\
&r_{\min} \cdot \sin\beta \leq z \leq \sqrt{r_{\min}^2 - x^2 - y^2}.
\end{aligned}$$

Proof Sketch. First, assume $\mathbf{x}_r$ is a closely reachable configuration of $\mathbf{x}$ and the translation part of $\mathbf{x}_r$ is p_r. According to the definition of closely reachable configurations, $\|p_r - p\|_2 \leq r_{\min}$, thus $p_r \in \text{cl}(\mathcal{B}(p, r_{\min}))$, where $\mathcal{B}(p, r_{\min})$ is

[1]M. Fu is with the Department of Computer Science, University of North Carolina at Chapel Hill, Chapel Hill, NC 27599, USA. mfu@cs.unc.edu

[*]Here, we make a common assumption that the needle body follows the tip, thus $\mathcal{X} \subset \mathcal{SE}(3)$ represents both 3D position and 3D orientation of the needle tip. Additionally, in the case for steerable needles, the needle can always rotate without insertion to achieve any desired roll angle, we do not explicitly mention this step in the following discussion.

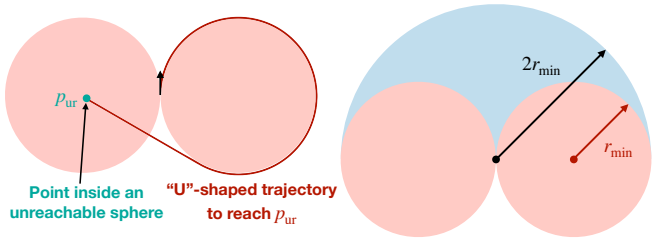

Fig. 2: Illustration of the forward reachable region. **Left:** Points inside an unreachable sphere are only reachable with "U"-shaped trajectories that are longer than $\pi r_{\min}$. **Right:** A visualization of the surfaces defining $\mathcal{R}^{\text{F}}$, $\mathcal{R}^{\text{F}}$ is shown as the blue-shaded region. The upper bound of β is π since the radius of $\mathcal{B}_{\text{ur}}(\alpha)$ equals to the radius of $\mathcal{B}(p, r_{\min})$.

the open sphere centered at p and with radius $r_{\min}$.

Now consider a trajectory leaving the the source configuration $\mathbf{x}$. For an arbitrary roll angle $\alpha \in [0, 2\pi)$, when the needle consistently takes the maximum curvature with out rotation, a circular arc trajectory is obtained on the plane $\sin\alpha \cdot x - \cos\alpha \cdot y = 0$. This is also the extreme case the needle could achieve, while any point inside $\mathcal{B}\left((r_{\min} \cdot \cos\alpha, r_{\min} \cdot \sin\alpha, 0), r_{\min}\right)$ is not reachable with trajectory length no longer than $\pi r_{\min}$ given curvature constraints.[†] See Fig. 2 for illustration.

Thus we have

$$p_r \in \mathcal{R}^{\text{F}} = \text{cl}(\mathcal{B}(p, r_{\min})) \cap \left(\mathbb{R}^3 \setminus \bigcup_{\alpha \in [0, 2\pi)} \mathcal{B}_{\text{ur}}(\alpha) \right) \cap \{(x, y, z) | z \geq 0\},$$

where $\mathcal{B}_{\text{ur}}(\alpha) = \mathcal{B}\left((r_{\min} \cdot \cos\alpha, r_{\min} \cdot \sin\alpha, 0), r_{\min}\right)$ is the (open) unreachable sphere determined by α. We require $z \geq 0$ since the initial orientation is facing positive z direction and we assume the needle only moves forward. As we can see in Fig. 2, the surface of the unreachable region $\cup_{\alpha \in [0,2\pi)} \mathcal{B}_{\text{ur}}(\alpha)$ is trumpet-shaped.

Finally, following our parameterization, the upper bound of β is π which corresponds to the intersecting curve of the two surfaces (see Fig. 2).

□

Similarly, we can have the backward reachable region, denoted as $\mathcal{R}^{\text{B}}$ that follows

$$\mathcal{R}^{\text{B}} = \text{cl}(\mathcal{B}(p, r_{\min})) \cap \left(\mathbb{R}^3 \setminus \bigcup_{\alpha \in [0, 2\pi)} \mathcal{B}_{\text{ur}}(\alpha) \right) \cap \{(x, y, z) | z \leq 0\}.$$

Fig. 1 provides visualization of the forward reachable region $\mathcal{R}^{\text{F}}$ and the backward reachable region $\mathcal{R}^{\text{B}}$ in 3D.[‡] We note that similar ideas of trumpet-shaped regions have been used in existing work on steerable needles, e.g. [2]–[4].

Note that the curve composed of centers of the unreachable spheres of is a circle. For example, for $\mathbf{x}$ with $p = (0, 0, 0)$ and $q = (1, 0, 0, 0)$, the circle can be written as

$$\forall \alpha \in [0, 2\pi),$$
$$x = r_{\min} \cdot \cos\alpha, y = r_{\min} \cdot \sin\alpha, z = 0.$$

For any configuration $\mathbf{x} = (p, q)$, we denote such circle as $\mathcal{C}^{\mathbf{x}}_{\text{center}}$. The normal vector of the trumpet surface at point $p' \in \mathbb{R}^3$ is the direction from the center of a corresponding sphere center to p'. Here, the corresponding sphere center of p' is the intersecting point of $\mathcal{C}^{\mathbf{x}}_{\text{center}}$ and the plane defined by q and p'. See Fig. 1 for illustration.

Next, consider two configrurations $\mathbf{x}_0, \mathbf{x}_1 \in \mathcal{X}$ with $\mathbf{x}_i = (p_i, q_i)$. To facilitate the following discussions, we denote the forward reachable region of $\mathbf{x}_0$ as $\mathcal{R}^{\text{F}}_0$, the backward reachable region of $\mathbf{x}_1$ as $\mathcal{R}^{\text{B}}_1$, and the trumpet surface of $\mathcal{R}^{\text{F}}_0$ as $\mathcal{S}^{\text{F}}_0$, and the trumpet surface of $\mathcal{R}^{\text{B}}_1$ as $\mathcal{S}^{\text{B}}_1$.

We now state the major theorem about close reachability.

Theorem 1. *For two configurations $\mathbf{x}_0, \mathbf{x}_1 \in \mathcal{X}$, $\mathbf{x}_1$ is closely reachable from $\mathbf{x}_0$ if and only if*

(i) $p_1 \in \mathcal{R}^{\text{F}}_0, p_0 \in \mathcal{R}^{\text{B}}_1$,

(ii) $\min\limits_{\alpha_1 \in [0,2\pi)} \left\{ \max\limits_{\alpha_0 \in [0,2\pi)} \|\mathcal{C}^{\mathbf{x_0}}_{\text{center}}(\alpha_0) - \mathcal{C}^{\mathbf{x_1}}_{\text{center}}(\alpha_1)\|_2 \right\} \geq 2 \cdot r_{\min}$.

Additionally, if $\mathbf{x}_1$ is closely reachable from $\mathbf{x}_0$, there exists a curvature bounded trajectory from $\mathbf{x}_0$ to $\mathbf{x}_1$ that is smooth and composed of three trajectory segments, with non-negative length, whose curvatures are $\kappa_{\max}, 0, \kappa_{\max}$, respectively.

Proof Sketch. We first prove that if $\mathbf{x}_1$ is closely reachable from $\mathbf{x}_0$, the two conditions (i) and (ii) above are satisfied. Intuitively, if $\mathbf{x}_1$ is closely reachable from $\mathbf{x}_0$, there exists some bounded-curvature trajectory σ_{cb} that satisfies $\forall s \in [0, \ell(\sigma_{\text{cb}})], \sigma_{\text{cb}}(s) \in \mathcal{R}^{\text{F}}_0 \cap \mathcal{R}^{\text{B}}_1$. This implies that if the intersection of $\mathcal{R}^{\text{F}}_0$ and $\mathcal{R}^{\text{B}}_1$ does not have a connection region that includes both p_0 and p_1, then there is no physical space for σ_{cb} to travel through from p_0 to p_1. Some examples and counter examples are shown in Fig. 3.

We now formalize this idea. According to Lem. 1, it is straightforward that the first condition, $p_1 \in \mathcal{R}^{\text{F}}_0, p_0 \in \mathcal{R}^{\text{B}}_1$, is necessary . For the second condition, we use proof by contradiction. Namely, if the second condition is not satisfied, it is not possible for $\mathbf{x}_1$ to be closely reachable from $\mathbf{x}_0$.

Here, $d = \|\mathcal{C}^{\mathbf{x_0}}_{\text{center}}(\alpha_0) - \mathcal{C}^{\mathbf{x_1}}_{\text{center}}(\alpha_1)\|_2$ is the Euclidean distance between the sphere centers of two unreachable regions, one for $\mathbf{x}_0$ and the other for $\mathbf{x}_1$. If $d > 2 \cdot r_{\min}$, the two spheres do not intersect; if $d = 2 \cdot r_{\min}$, the two spheres are tangent; and if $d < 2 \cdot r_{\min}$, the two spheres are intersecting. Denote

$$d^* = \min_{\alpha_1 \in [0,2\pi)} \left\{ \max_{\alpha_0 \in [0,2\pi)} \|\mathcal{C}^{\mathbf{x_0}}_{\text{center}}(\alpha_0) - \mathcal{C}^{\mathbf{x_1}}_{\text{center}}(\alpha_1)\|_2 \right\}.$$

If $d^* < 2 \cdot r_{\min}$, there must exists one unreachable sphere centered at $\mathcal{C}^{\mathbf{x_1}}_{\text{center}}(\alpha^*_1)$ (corresponding to d^*) that intersects with spheres centered at every $\mathcal{C}^{\mathbf{x_0}}_{\text{center}}(\alpha_0), \forall \alpha_0 \in [0, 2\pi)$. This indicates that all possible trajectories in $\mathcal{R}^{\text{F}}_0$ from p_0

[†]This idea follows the Pestov–Ionin theorem [1].

[‡]For simplicity, in figures in this section, we only show the trumpet surface without the upper bound for z.

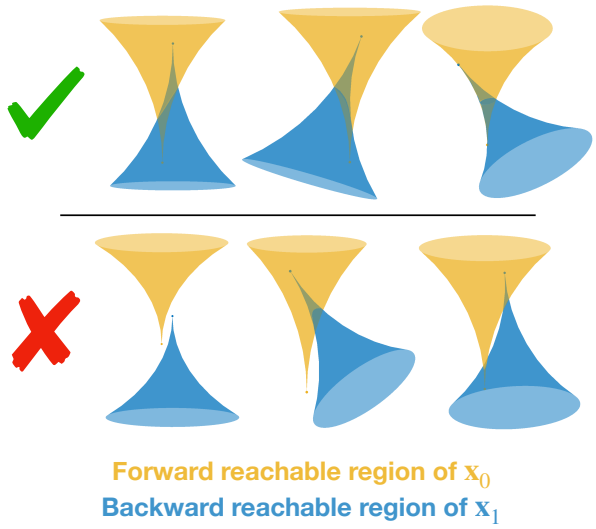

Fig. 3: Examples of closely reachable configurations (top) and non-closely reachable configurations (bottom). In the bottom examples, $\mathbf{x}_1$ is not reachable because (i) both p_0 and p_1 are not in the reachable region; (ii) p_0 or p_1 is not in the reachable region; or (iii) although both p_0 and p_1 are in the reachable region, the intersection of the two reachable regions does not connect p_0 and p_1.

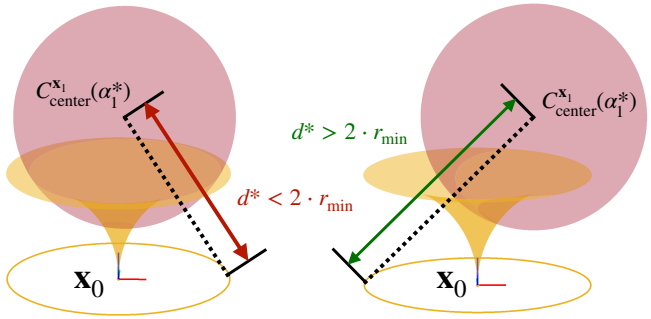

Fig. 4: Example of a closely reachable case and a closely unreachable case, considering d^* and $C^{\mathbf{x}_1}_{\text{center}}(\alpha_1^*)$.

will enter an unreachable sphere of $\mathbf{x}_1$ before reaching p_1.[§] See Fig. 4. Thus $\mathbf{x}_1$ is not closely reachable from $\mathbf{x}_0$.

We now prove that if both conditions (i) and (ii) hold, $\mathbf{x}_1$ is closely reachable from $\mathbf{x}_0$. We approach this by constructing a trajectory from $\mathbf{x}_0$ to $\mathbf{x}_1$, composed of three trajectory segments whose curvatures are $\kappa_{\max}, 0, \kappa_{\max}$, respectively. If such trajectory exists, $\mathbf{x}_1$ is by definition closely reachable.

This proof relies on a physical model of an ideal elastic rubber string. That is, consider the scenario where we have an elastic rubber string whose ends are firmly attached to the 3D positions p_0 and p_1 respectively. Our idea is to analyze this physical system and find the shape of the elastic rubber string (when there exist trumpet surfaces that enforce the orientations and curvature constraints as detailed later), which also indicates a trajectory σ_s that goes from $\mathbf{x}_0$ to its closely reachable configuration $\mathbf{x}_1$. If σ_s satisfies the three-segment condition, the lemma is proved.

[§]It is also not possible for p_1 to lie on the sphere surface that is exposed to $\mathbf{x}_0$, since if that is the case, the sphere centered at $C^{\mathbf{x}_1}_{\text{center}}(\alpha_1^* + \pi)$ would produce a smaller d^* and violates the construction of α_1^*.

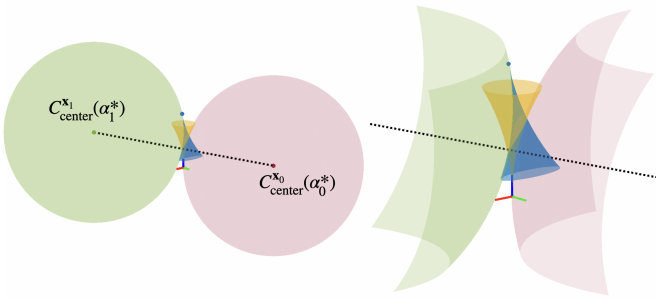

Fig. 5: The two unreachable spheres defining the minimum gap. With $d^* - 2 \cdot r_{\min} \geq 0$, the intersection $\mathcal{R}_0^{\mathrm{F}} \cap \mathcal{R}_1^{\mathrm{B}}$ forms a physical space from $\mathbf{x}_0$ to $\mathbf{x}_1$.

We now state the detailed assumptions for the physical system. We first assume the elastic rubber string is fully stretched, infinitely thin, and zero-weighted. If a string is fully stretched, at each point along the string, there exists internal tension applied in the direction along the string. To model the curvature constraints, we assume p_0 and p_1 each is associated with one trumpet surface, representing the boundary of the forward reachable region and the backward reachable region, respectively. We then assume these trumpet surfaces $\mathcal{S}_0$ and $\mathcal{S}_1$ are solid, support the elastic rubber string and have perfectly-zero friction. These assumptions indicate that the trumpet surfaces can apply forces to the rubber string only in normal directions. We finally assume there is no other external force sources, such as gravity and buoyancy.

Before analyzing the shape of the rubber string, we note that the geometrical meaning of $d^* - 2 \cdot r_{\min}$ is the minimum gap between unreachable region of $\mathbf{x}_0$ and $\mathbf{x}_1$. With a non-negative minimum gap, there exists a connected physical space for the string to travel through. See Fig. 5 for illustration.

We now analyze the shape of the rubber string and we consider two different cases separately.

Case 1: at least one of p_0 and p_1 is on $\mathcal{S}_0 \cap \mathcal{S}_1$. Note that by construction p_0 is on $\mathcal{S}_0$ and p_1 is on $\mathcal{S}_1$. Thus $p_0 \in \mathcal{S}_0 \cap \mathcal{S}_1$ indicates p_0 is also on $\mathcal{S}_1$.

We prove that as long as one point in p_0 and p_1 is on $\mathcal{S}_0 \cap \mathcal{S}_1$, the other point in the two is also on $\mathcal{S}_0 \cap \mathcal{S}_1$. Here we only show that if $p_0 \in \mathcal{S}_0 \cap \mathcal{S}_1$, then $p_1 \in \mathcal{S}_0 \cap \mathcal{S}_1$. The case with $p_1 \in \mathcal{S}_0 \cap \mathcal{S}_1$ can be proved symmetrically.

As $p_0 \in \mathcal{S}_1$, we are able to find the unreachable sphere, denoted as $\mathcal{B}_{\text{ur}}(\mathcal{S}_1, p_0)$, that is associated with p_0, and the normal vector for $\mathcal{S}_1$ at p_0 is denoted as $\mathbf{v}(\mathcal{S}_1, p_0)$. Note by construction p_1 is on the surface of $\mathcal{B}_{\text{ur}}(\mathcal{S}_1, p_0)$. We have $p_1 \in \mathcal{R}_0$ to guarantee p_1 reachable from $\mathbf{x}_0$, so either $p_1 \in \mathcal{S}_0$ or $p_1 \in \mathcal{R}_0 \setminus \mathcal{S}_0$. If $p_1 \in \mathcal{R}_0 \setminus \mathcal{S}_0$, the unreachable sphere $\mathcal{B}_{\text{ur}}(\mathcal{S}_1, p_0)$ and the forward reachable region $\mathcal{R}_0$ has non-empty intersection and the direction vector of q_0 is pointing inside $\mathcal{B}_{\text{ur}}(\mathcal{S}_1, p_0)$ (see Fig. 6). This cause there to be no connected region in $\mathcal{R}_0 \cap \mathcal{R}_1$ that contains p_0 and p_1, which violates the definition of closely reachable configuration. So it is only possible to have $p_1 \in \mathcal{S}_0$ and $\mathcal{B}_{\text{ur}}(\mathcal{S}_1, p_0)$ tangent to $\mathcal{S}_0$ (See Fig. 6). As the maximum-curvature arc from p_0 to p_1 on the surface of $\mathcal{B}_{\text{ur}}(\mathcal{S}_1, p_0)$ is on both $\mathcal{S}_0$ and $\mathcal{S}_1$,

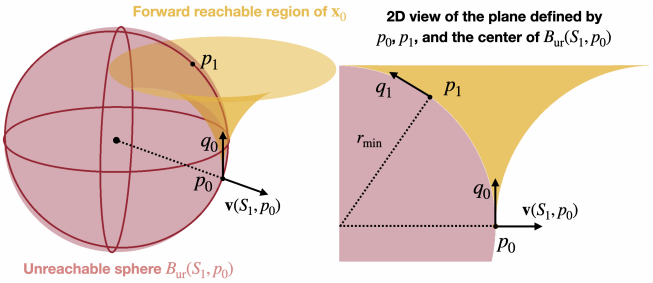

Fig. 6: Illustration for case 1 that if $p_0 \in \mathcal{S}_0 \cap \mathcal{S}_1$, then $p_1 \in \mathcal{S}_0 \cap \mathcal{S}_1$.

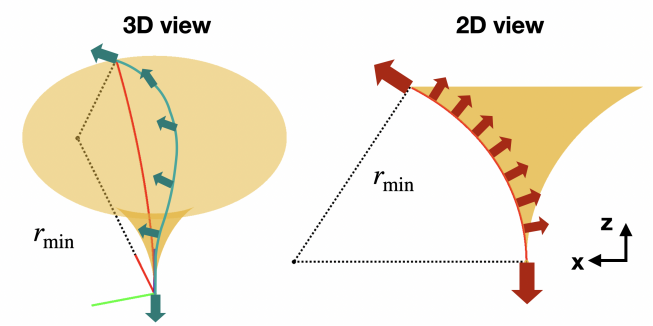

Fig. 7: Force analysis for a string segment where external force applied to the segment is shown in thick arrows. The red line shows a stable (possible) string shape while the dark green line shows an unstable string shape. Without losing generality, we assume the free end of the segment lies in the X-Z plane. And we can see that for the unstable case, the overall force the trumpet applies to the string has a positive Y component which no other force can compensate. Thus the force applied to the segment is not balanced and the string shape is unstable. Note it is possible to have all external force balanced if the string takes a "S" shape, but we can do similar analysis for its sub-segments and conclude that the shape is still unstable.

it is straight forward that we have one maximum-curvature arc connecting $\mathbf{x}_0$ and $\mathbf{x}_1$ as the first segment, and the other two segments have zero length.

Case 2: p_1 is not on $\mathcal{S}_0$ and p_0 is not on $\mathcal{S}_1$. Recall that by construction p_0 is on $\mathcal{S}_0$ and p_1 is on $\mathcal{S}_1$. Since σ_s connects p_0 and p_1, there exist two points represented by $t_0, t_1 \in [0, \ell(\sigma_s)]$ where $\sigma_s(t_0)$ is the last point that the string is on $\mathcal{S}_0$ while $\sigma_s(t_1)$ is the first point that the string is on $\mathcal{S}_1$. We take the string segment $[0, t]$ as one complete object. Here, $t = \min(t_0, t_1)$ is denoted as the *transition point*. According to the force analysis in Fig. 7, since it is impossible to have friction to compensate for any "sideward" forces, the segment must follow a maximum-curvature arc and the direction of the string at $\sigma_s(t)$ follows the tangent direction. Since we can also follow the string from p_1 to p_0, symmetrically, we do the same analysis for the segment $[t', \ell(\sigma_s)]$ where t' is a similar transition point for p_1.

We have shown the segments $[0, t]$ and $[t', \ell(\sigma_s)]$ are maximum-curvature arcs, we now focus on the middle segment $[t, t']$. By construction, we have $t \leq t'$. There are three possible conditions:

(i) $t = t'$. This indicates the middle segment has zero length, the three-segment condition is met. Since there's no friction, the string is smooth at the transition point.

(ii) $t < t'$ and $\sigma_s(t) \notin \mathcal{S}_1, \sigma_s(t') \notin \mathcal{S}_0$. Without any other external force, once the string detaches from $\mathcal{S}_0$, it won't come back to $\mathcal{S}_0$ unless $\mathcal{S}_1$ pushes it to do so, but the string won't touch $\mathcal{S}_1$ until point t', thus the segment (t, t') is not on either of the trumpet surfaces. As there's no other external force other than the tension applied to the segment at the two transition points, the string forms a straight line. And the string is smooth at the transition points since there's no friction. The middle segment is with curvature 0 and the three-segment condition is met.

(iii) $t < t'$ and at least one of $\sigma_s(t)$ and $\sigma_s(t')$ is on $\mathcal{S}_0 \cap \mathcal{S}_1$. Take $\sigma_s(t) \in \mathcal{S}_0 \cap \mathcal{S}_1$ as an example. Denote the string direction at $\sigma_s(t)$ as a vector $\mathbf{d}(t)$. To $\mathbf{d}(t)$ as is, the normal direction $\mathbf{v}(\mathcal{S}_1, \sigma_s(t))$ has to be perpendicular to $\mathbf{d}(t)$. Then all possible cases for the unreachable sphere $\mathcal{B}_{\text{ur}}(\mathcal{S}_1, \sigma_s(t))$ forms a new trumpet, on whose surface lie all possible positions for p_1. Since the new trumpet region is a subset of $\mathcal{R}_0$, the maximum-curvature arc from $\sigma_s(t)$ to p_1 on $\mathcal{B}_{\text{ur}}(\mathcal{S}_1, \sigma_s(t))$ dose not intersect with $\mathcal{S}_0$. So the string would follow such maximum-curvature arc as $\mathcal{S}_0$ won't apply any force to the segment to deviate. But this in return indicates $t = t'$ which conflicts with the initial assumption. Thus, this final condition is impossible.

From the above discussion, we have shown that a curvature-bounded trajectory from $\mathbf{x}_0$ to $\mathbf{x}_1$ exists. Recall that the definition of closely reachable configuration further requires the Euclidean distance between p_0 and p_1 is no larger than $r_{\min}$ and the trajectory length is no larger than $2 \cdot r_{\min}$. The first condition, $p_1 \in \mathcal{R}_0^{\text{F}}, p_0 \in \mathcal{R}_1^{\text{B}}$, guarantees that $\|p_0 - p_1\|_2 \leq 2r_{\min}$. And since trajectory σ_s lives in $\mathcal{R}_0^{\text{F}} \cap \mathcal{R}_1^{\text{B}}$ and with curvature bounded by $\kappa_{\max}$, the maximum possible trajectory length is $\pi r_{\min}$.

In conclusion of all above, the lemma is proved. □

II. A Numerical Method to Compute Bounded-Curvature Trajectories

A. Check for close-range reachability

Our proposed method works when a configuration is actually closely reachable. So for any given pair of configurations, we first check if close-range reachability holds. Following Thm. 1, we just need to check if both conditions are satisfied. Details is described in Alg. 1.

In Alg. 1 line 3-10, we first check for Thm. 1 condition (i). In Alg. 1 line 11-16and check for Thm. 1 condition (ii). Details for Alg. 1 line 14 is illustrated in Fig. 9.

Since we are checking if the minimum d is smaller than $2r_{\min}$, we just need to find one α that satisfies line 14-15.

B. Compute a bounded-curvature connection

With the above lemma, we are able to compute the three-segment trajectories for some examples of closely reachable configurations (See Fig. 8).

Alg. 2 shows our algorithm to compute the connection. Here, we compute two *transition points* t_0, t_1, together with $\mathbf{x}_0$ and $\mathbf{x}_1$, a three-segment connection is defined.

Generally speaking, we iteratively update transition points t_0 and t_1 until they both converge to a stable state with an error lower than a predefined threshold ε.

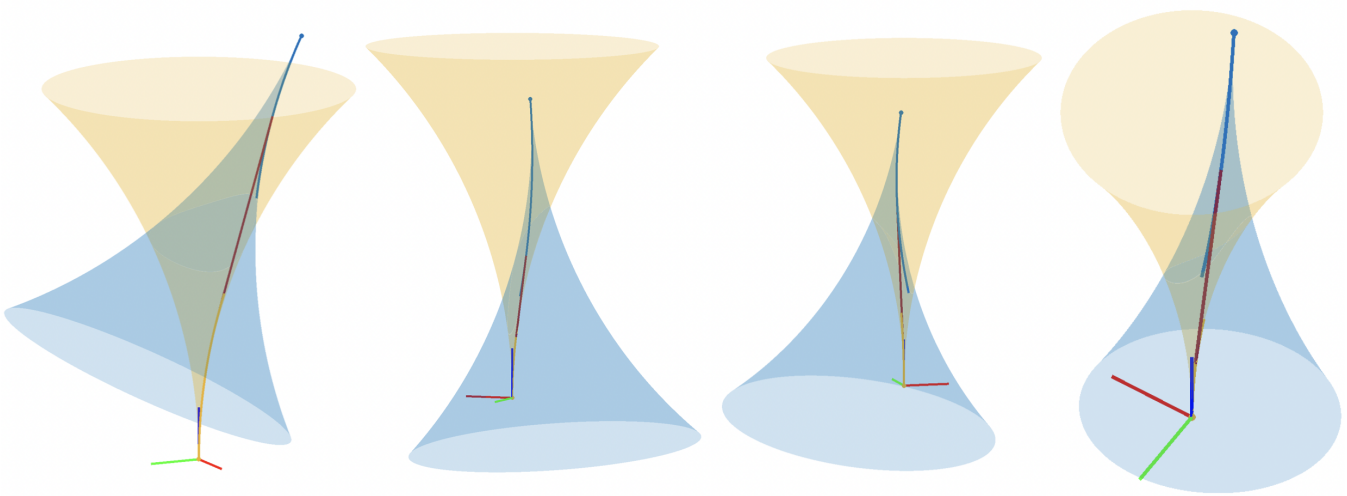

Fig. 8: Example of the three-segment trajectories for closely reachable configurations. Three segments are shown in yellow, red, and blue respectively. The maximum curvature segments are intentionally plotted longer (beyond the tangent point) to show the middle segment is tangent to the maximum curvature segments at the transition points.

Algorithm 1 CloseRangeReachabilityCheck

Input: $\mathbf{x}_0, \mathbf{x}_1, r_{\min}$

1: $\delta \leftarrow 0.01$ ▷ Define the check resolution
2: $p_0 \leftarrow \text{Pos}(\mathbf{x}_0), p_1 \leftarrow \text{Pos}(\mathbf{x}_1)$
3: **if** $\|p_0 - p_1\|_2 > 2r_{\min}$ **then**
4: **return** False ▷ Violates the first condition in Def. 1
5: $\mathcal{P}_{01} \leftarrow \text{DefinePlane}(\mathbf{x}_0, p_1)$
6: **if** $\|p_1 - (\mathcal{P}_{01} \cap \mathcal{C}^{\mathbf{x}_0}_{\text{center}})\|_2 < r_{\min}$ **then**
7: **return** False ▷ Inside an unreachable sphere
8: $\mathcal{P}_{10} \leftarrow \text{DefinePlane}(\mathbf{x}_1, p_0)$
9: **if** $\|p_0 - (\mathcal{P}_{10} \cap \mathcal{C}^{\mathbf{x}_1}_{\text{center}})\|_2 < r_{\min}$ **then**
10: **return** False ▷ Inside an unreachable sphere
11: $\mathcal{P}_0 \leftarrow \text{DefinePlane}(\mathcal{C}^{\mathbf{x}_0}_{\text{center}})$
12: **for** $\alpha \in \{0, \delta, 2\delta, \ldots, n\delta\}$, where $n = \lceil \frac{2\pi}{\delta} \rceil$ **do**
13: $p'_1 \leftarrow \text{Project}(\mathcal{C}^{\mathbf{x}_1}_{\text{center}}(\alpha), \mathcal{P}_0)$ ▷ Project a point onto a plane
14: $d = \sqrt{\|\mathcal{C}^{\mathbf{x}_1}_{\text{center}}(\alpha) - p'_1\|_2^2 + (r_{\min} + \|p_0 - p'_1\|_2)^2}$
15: **if** $d < 2r_{\min}$ **then**
16: **return** False ▷ Violates the second condition in Thm. 1
17: **return** True

Alg. 2 line 5 and 8 both call a function that computes a 2D Dubins path that starts from an orientation constrained configuration and ends at an orientation unconstrained 3D point. Here, we consider the Dubins path to start with a maximum curvature segment, following a straight-line segment. Function Shortest2D$(\cdot)$ is detailed in Alg. 3 and Fig. 10.

III. Conclusion

We see this method to be a building block for potential motion planners for medical steerable needles. With the theorem and method we provide, we can do local connections between configurations, thus making PRM and RRT*

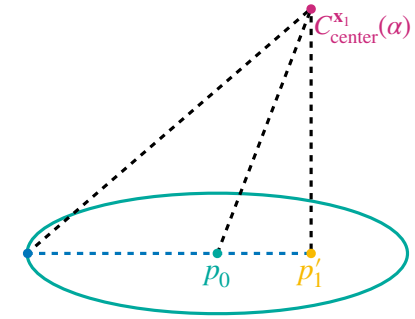

Fig. 9: Consider the case of computing the furthest distance from a point, $p = \mathcal{C}^{\mathbf{x}_1}_{\text{center}}(\alpha)$, to a circle, $\mathcal{C}^{\mathbf{x}_0}_{\text{center}}$, on a plane. The distance from p to any point along the circle equals to $\sqrt{h^2 + d^2}$, where $h = \|p - p'_1\|_2$ is the distance from p to the plane and d is the distance from p'_1 to the point along the circle. Clearly, h is a constant for a given scenario and the maximum distance is achieved along the straight line defined by p'_1 and p_0 since $\|p'_1 - \mathcal{C}^{\mathbf{x}_0}_{\text{center}}(\beta)\|_2 \leq \|p'_1 - p_0\|_2 + r_{\min}$.

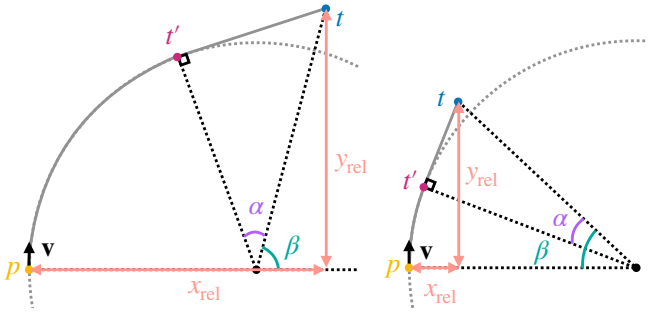

Fig. 10: Illustration of function Shortest2D$(\cdot)$. Since a plane is uniquely defined by $\mathbf{x}$ and t (set aside the singular case where $\vec{pt} = \lambda \text{Tangent}(\mathbf{x})$), the trajectory $p \rightarrow t' \rightarrow t$ can be deterministically computed. Refer to Alg. 3 for detailed computation.

Algorithm 2 ComputeBoundedCurvatureConnection
Input: $\mathbf{x}_0, \mathbf{x}_1, r_{\min}$

$\varepsilon \leftarrow 1e^{-6}$ ▷ Define the error threshold
$t_0 \leftarrow \text{Pos}(\mathbf{x}_0), t_1 \leftarrow \text{Pos}(\mathbf{x}_1)$ ▷ Initialize transition points
while True **do**
  $t_0^{\text{tmp}} \leftarrow \text{Shortest2D}(\mathbf{x}_0, t_1, r_{\min})$
  $\varepsilon_0 \leftarrow \|t_0 - t_0^{\text{tmp}}\|_2$, $t_0 \leftarrow t_0^{\text{tmp}}$
  $t_1^{\text{tmp}} \leftarrow \text{Shortest2D}(\mathbf{x}_1, t_0, r_{\min})$
  $\varepsilon_1 \leftarrow \|t_1 - t_1^{\text{tmp}}\|_2$, $t_1 \leftarrow t_1^{\text{tmp}}$
  if $\varepsilon_0 \leq \varepsilon$ **and** $\varepsilon_1 \leq \varepsilon$ **then**
    break
return $\{t_1, t_2\}$

Algorithm 3 Shortest2D
Input: $\mathbf{x}, t, r_{\min}$

$p \leftarrow \text{Pos}(\mathbf{x})$, $\mathbf{v} \leftarrow \text{Tangent}(\mathbf{x})$ ▷ Get position and orientation
if $\vec{pt} = \lambda \mathbf{v}$ for $\lambda \in \mathbb{R}$ **then**
  return p ▷ Singular case
$y_{\text{rel}} = \text{dot}(\mathbf{v}, \vec{pt})$
if $y_{\text{rel}} < 0$ **then**
  $y_{\text{rel}} \leftarrow -y_{\text{rel}}$
  $\mathbf{v} \leftarrow -\mathbf{v}$
$\mathbf{v}_c = \text{Normalize}(\vec{pt} - y_{\text{rel}} \cdot \mathbf{v})$
$x_{\text{rel}} \leftarrow \sqrt{\|p - t\|_2^2 - y_{\text{rel}}^2}$
$d \leftarrow \sqrt{y_{\text{rel}}^2 + (x_{\text{rel}} - r_{\min})^2}$
$\alpha \leftarrow \arccos(\frac{r_{\min}}{d}), \beta \leftarrow \arcsin(\frac{y_{\text{rel}}}{d})$
if $x_{\text{rel}} < r_{\min}$ **then**
  $\theta \leftarrow \beta - \alpha$
else
  $\theta \leftarrow \pi - \beta - \alpha$
if $\theta < \frac{\pi}{2}$ **then**
  $\delta x \leftarrow r_{\min}(1 - \cos\theta), \delta y \leftarrow r_{\min} \sin\theta$
else
  $\delta x \leftarrow r_{\min}(1 + \cos\theta), \delta y \leftarrow r_{\min} \sin\theta$
$t' \leftarrow p + \delta x \cdot \mathbf{v}_c + \delta y \cdot \mathbf{v}$
return t'

style planners to be directly applicable to steerable needles. Additionally, the theorem we provide might also serve as a validation method, when the start and goal orientations are constrained.

REFERENCES

[1] V. Ionin and G. Pestov, "On the largest possible circle imbedded in a given closed curve," in *Proceedings of the USSR Academy of Sciences (in Russian)*, vol. 127, 1959, pp. 1170–1172.

[2] A. Favaro, A. Segato, F. Muretti, and E. D. Momi, "An evolutionary-optimized surgical path planner for a programmable bevel-tip needle," *IEEE Trans. Robotics*, vol. 37, no. 4, pp. 1039–1050, 2021.

[3] M. Pinzi, T. Watts, R. Secoli, S. Galvan, and F. R. y. Baena, "Path replanning for orientation-constrained needle steering," *IEEE Trans. Biomedical Engineering*, vol. 68, no. 5, pp. 1459–1466, 2021.

[4] J. Hoelscher, M. Fu, I. Fried, M. Emerson, T. E. Ertop, M. Rox, A. Kuntz, J. A. Akulian, R. J. Webster III, and R. Alterovitz, "Backward planning for a multi-stage steerable needle lung robot," *IEEE Robotics and Automation Letters*, vol. 6, no. 2, pp. 3987–3994, 2021.